

CheY's acetylation sites responsible for generating clockwise flagellar rotation in *Escherichia coli*

Milana Fraiberg,¹ Oshri Afanzar,¹ C. Keith Cassidy,² Alexandra Gabashvili,³ Klaus Schulten,² Yishai Levin³ and Michael Eisenbach^{1*}

¹Department of Biological Chemistry, The Weizmann Institute of Science, 7610001 Rehovot, Israel.

²Department of Physics, University of Illinois at Urbana-Champaign, Urbana, IL 61801, USA.

³de Botton Institute for Protein Profiling, The Nancy and Stephen Grand Israel National Center for Personalized Medicine, The Weizmann Institute of Science, 7610001 Rehovot, Israel.

Summary

Stimulation of *Escherichia coli* with acetate elevates the acetylation level of the chemotaxis response regulator CheY. This elevation, in an unknown mechanism, activates CheY to generate clockwise rotation. Here, using quantitative selective reaction monitoring mass spectrometry and high-resolution targeted mass spectrometry, we identified K91 and K109 as the major sites whose acetylation level *in vivo* increases in response to acetate. Employing single and multiple lysine replacements in CheY, we found that K91 and K109 are also the sites mainly responsible for acetate-dependent clockwise generation. Furthermore, we showed that clockwise rotation is repressed when residue K91 is nonmodified, as evidenced by an increased ability of CheY to generate clockwise rotation when K91 was acetylated or replaced by specific amino acids. Using molecular dynamics simulations, we show that K91 repression is manifested in the conformational dynamics of the $\beta 4\alpha 4$ loop, shifted toward an active state upon mutation. Removal of $\beta 4\alpha 4$ loop repression may represent a general activation mechanism in CheY, pertaining also to the canonical phosphorylation activation pathway as suggested by crystal structures of active and inactive CheY from *Thermotoga maritima*. By way of elimination, we

further suggest that K109 acetylation is actively involved in generating clockwise rotation.

Introduction

Acetylation of proteins on lysine residues (*N*-acetylation), a reversible post-translational covalent modification that adds an acetyl group to the ϵ -amino group of a lysine residue, is widespread in nature, from bacteria to mammals (Jones and O'Connor, 2011; Kim and Yang, 2011; Thao and Escalante-Semerena, 2011). In *Escherichia coli* alone, more than 100 proteins undergo *N*-acetylation. One of them, among the first to be identified as acetylatable, is the excitatory response regulator of chemotaxis, CheY (Barak *et al.*, 1992; 2004; 2006; Yan *et al.*, 2008). This protein undergoes acetylation by at least two mechanisms: acetylation by the enzyme acetyl-CoA synthetase (Acs) with acetate as an acetyl donor (Barak *et al.*, 1992; 2004) and autoacetylation with AcCoA as an acetyl donor (Barak *et al.*, 2006). CheY was found *in vitro* to be acetylated by each of these mechanisms at six acetylation sites: lysine residues 91, 92, 109, 119, 122 and 126 (Ramakrishnan *et al.*, 1998; Barak *et al.*, 2004; Barak *et al.*, 2006; Li *et al.*, 2010). The main function, shown thus far for CheY acetylation by Acs, is shifting the direction of flagellar rotation from the default, counterclockwise, to clockwise. This function, termed hereafter 'acetate-dependent clockwise generation', is observed even in the absence of the chemotaxis machinery. Thus, acetate addition to gutted cells expressing CheY from a plasmid but lacking all other chemotaxis proteins and some of the receptors (Wolfe *et al.*, 1988; Barak *et al.*, 1998; Ramakrishnan *et al.*, 1998) or to cytoplasm-free cell envelopes containing Acs (Barak *et al.*, 1992) resulted in prolonged clockwise rotation. Indeed, the acetylation level of CheY *in vivo* is high (Yan *et al.*, 2008), but it is not known which of the sites are affected by acetate and, accordingly, which of them is likely to be responsible for clockwise generation. Here, we identified that these sites are K91 and K109. Furthermore, the use of gutted cells fully devoid of the phosphorelay machinery uniquely enabled us to study, without perturbations of phosphorylation-dependent signaling, how subtle modifications in CheY activate the protein to generate clockwise rotation.

Accepted 6 November, 2014. *For correspondence. E-mail m.eisenbach@weizmann.ac.il; Tel. (+972) 8 9343923; Fax: (+972) 8 9342722.

Table 1. Acetylation sites of CheY *in vivo* revealed from MS/MS analyses.

Peptide sequence	Acetylation site on CheY ^a	MH ⁺ [Da] ^b	Xcorr ^c
Wild-type level of CheY (no IPTG) ATLEEKLN acK IF acK LG acK MGLCG	K122; K126	2351.21573	2.2
Wild-type level of CheY (no IPTG) + acetate HHTDPALRAAD acK EL acK DALNKLQAGGYGFVSDWNMPNMDGLELL acK TIR acK KENIIAAAQAG LMVTAE acK AC acK ENIIAAAQAGASG LN acK IF acK	K4; K7 K70 K91 K92 K122	1785.91252 3724.82656 1328.71623 2202.14408 933.53984	2.36 3.16 2.06 2.11 2.75
Elevated levels of CheY (IPTG) VV acK PF acK TAATLEEKLNK LEE acK LNKI TAATLEE acK LNKIF acK	K109 K119 K119; K126	1830.02666 1028.59380 1933.04265	3.21 1.91 1.86
Elevated levels of CheY (IPTG) + acetate ALPVLMTAE acK ENIIAAAQ VV acK PF acK TAATLEEKLNK LEE acK LNKI TAATLEE acK LNKIF acK	K91 K109 K119 K119; K126	2240.21514 1830.02666 1028.59380 1933.0265	2.17 3.07 1.98 1.92

a. According to protein accession P0AE67. The sites were determined according to acetylated peptides obtained by proteolytic digestion with trypsin and chymotrypsin.

b. MH⁺ is the mass of the protonated form of the peptide.

c. Xcorr is a cross-correlation score function calculated to assess the quality of the match between a tandem mass spectrum and amino acid sequence information in a database (Eng *et al.*, 1994). The peptides were identified using the Sequest search engine.

Results

To identify the acetylation site(s) responsible for clockwise generation, we first determined which of the acetylation sites is more often acetylated *in vivo* and influenced by acetate, and then examined whether this site is, indeed, involved in clockwise generation.

Acetylation sites of CheY *in vivo*

To identify the acetylation sites of CheY *in vivo*, we exposed extracts of *E. coli* Δ *cheY* cells expressing 6xHis-CheY from a plasmid to SDS polyacrylamide gel electrophoresis. We studied two expression levels of CheY. One without induction produces a relatively low level of CheY as judged by both Western blots (Supporting Information Fig. S1) and functional assays of expanding ring formation on semisolid agar (Adler, 1966; Fig. S2). The other was with induction by isopropyl β -D-thiogalactopyranoside (IPTG; 1 mM), making the detection easier (Fig. S1). We subjected the CheY gel bands to shotgun proteomics using tandem mass spectrometry (MS/MS). We performed in-gel digestion using trypsin and chymotrypsin, which yielded a mixture of peptides for each gel band. We analyzed these mixtures by high-resolution tandem mass spectrometry, which facilitates identification of the CheY peptides through collision-induced dissociation in the instrument. This resulted in peptide fragmentation spectra also used for identification of acetylation sites on the peptide sequences. The analysis identified essentially all the sites known to be acetylated *in*

vitro and, in addition, lysine residues 4, 7 and 70 (Table 1, Fig. S3). Yet it only provided a qualitative view of CheY acetylation *in vivo*.

K91 and K109 are the sites most affected by acetate in vivo

To determine the quantitative differences between the acetylation levels in the various sites and to establish the effect of acetate on these levels, we used synthetic acetylated standard peptides combined with quantitative, selective reaction monitoring (SRM) mass spectrometry, an established approach for quantification of peptides and proteins in complex biological samples (Addona *et al.*, 2009). We first separated proteins from each of the samples by SDS-PAGE and then subjected the relevant bands to SRM. Using this method in conjunction with synthetic, acetylated peptide standards (Table S1), we obtained absolute concentrations of the targeted acetylated peptides. We mainly relied on peptides obtained from IPTG-induced CheY (Table 2) because more peptides at higher levels of expression could be detected. Excluding the K45-containing peptide (see below), whenever peptides from noninduced CheY could be detected (Table S2), they were those already obtained from induced CheY (Table 2). Although we found lysine residues 26, 45, 91, 92, 122 and 126 to be acetylated, there were some batch-to-batch differences. For example, K126 was only detected in batch 3 (Table 2), and K45 was only detected in samples without IPTG (Table S2).

Table 2. Low-resolution targeted mass spectrometry measurements of lysine acetylated residues on CheY^a with and without acetate.

Peptide sequence	Acetylation site on CheY	Acetylated peptides [pM]	
		Absence of acetate	Presence of acetate
Experiment I			
NLLacKELGFNNVEEAEDGVDALNK	K26	28.9	68.2
TIRADGAMSALPVLMTAEAcK	K91	0	52.2
ADGAMSALPVLMTAEAcKacK	K91, K92	0.03	0.52
LNacKIFEK	K122	0.4	13.35
Experiment II			
NLLacKELGFNNVEEAEDGVDALNK	K26	5.4	6.4
TIRADGAMSALPVLMTAEAcK	K91	0	137.05
LNacKIFEK	K122	0.42	13.35
Experiment III			
IVRNLLacK	K26	3.2	1.7
NLLacKELGFNNVEEAEDGVDALNK	K26	2.5	0.3
TIRADGAMSALPVLMTAEAcK	K91	142.2	322.3
LNacKIFEK	K122	5942.3	2793.3
LNKIFEacK	K126	3940.2	4692.3
LNacKIFEacK	K122; K126	128.5	261.3

a. IPTG-induced CheY.

To determine the effect of acetate on the acetylation sites, we supplemented portions of the same cultures with acetate for 1 h growth prior to harvesting. The only acetylation site that showed a consistent change in the acetylation level in response to acetate was K91, whose level consistently increased (Fig. 1 and Table 2). However, these low-resolution targeted mass spectrometry measurements could not detect acetylation on residues K109 and K119, if occurred. This is because there is no trypsin digestion site between them (i.e., unmodified Lys or Arg), meaning that the resulting peptides after protein digestion were too long for analysis by mass spectrometry.

To circumvent this difficulty, we digested the IPTG-induced samples by both trypsin and chymotrypsin, and then employed high-resolution targeted mass spectrometry measurements, which enabled relative quantification of the acetylation ratios prior and subsequent to treatment with acetate. With this approach, we identified four different peptides containing acetylated K109 (Table 3). The

Table 3. High-resolution targeted mass spectrometry measurements of K109 and K119 on CheY with and without acetate.

Peptide sequence	Site on CheY	Acetate (+/-) ratio
KENIIAAQAGASGYVvacK	K109	1.55
KENIIAAQAGASGYVvacKPF	K109	1.51
ENIIAAQAGASGYVvacKPFTAATL	K109	2.56
VvacKPFTAATLEEK	K109	2.46
TAATLEEacKLNK	K119	1.01

acetylation levels of all of them were consistently elevated (doubled on average) in response to acetate (Fig. 2 and Table 3). Even though acetylation of K119 was detected as well, its level did not change in response to acetate treatment (Table 3). Thus, *in vivo*, acetate treatment predominantly results in K91 and K109 acetylation, suggesting that these two sites are responsible for the acetate-dependent clockwise generation.

K91 and K109 are responsible for the acetate-dependent clockwise generation

To examine this possibility, we prepared by site-directed mutagenesis arginine-for-lysine replacement mutants at sites 91 and 109. As controls, we similarly prepared KR replacements at the other previously identified acetylation sites: K92, K119, K122 and K126. [A KR replacement conserves the positive electric charge but does not undergo acetylation (Li *et al.*, 2002; Kim and Yang, 2011).] We expressed the CheY mutant proteins to a low level (without IPTG) in a gutted background (mentioned under *Experimental Procedures*), thus avoiding a repellent response to acetate (Wolfe *et al.*, 1988). Furthermore, to prevent the generation of acetyl phosphate, which can generate clockwise rotation by phosphorylating CheY, all the gutted strains were also deleted for both *ack* and *pta* (encoding acetate kinase and phosphotransacetylase respectively) (Barak *et al.*, 1998). To examine the ability of acetate to generate clockwise rotation in the mutants, we tethered the cells to glass slides via their flagella and looked for changes in the direction of flagellar rotation in response to acetate addition.

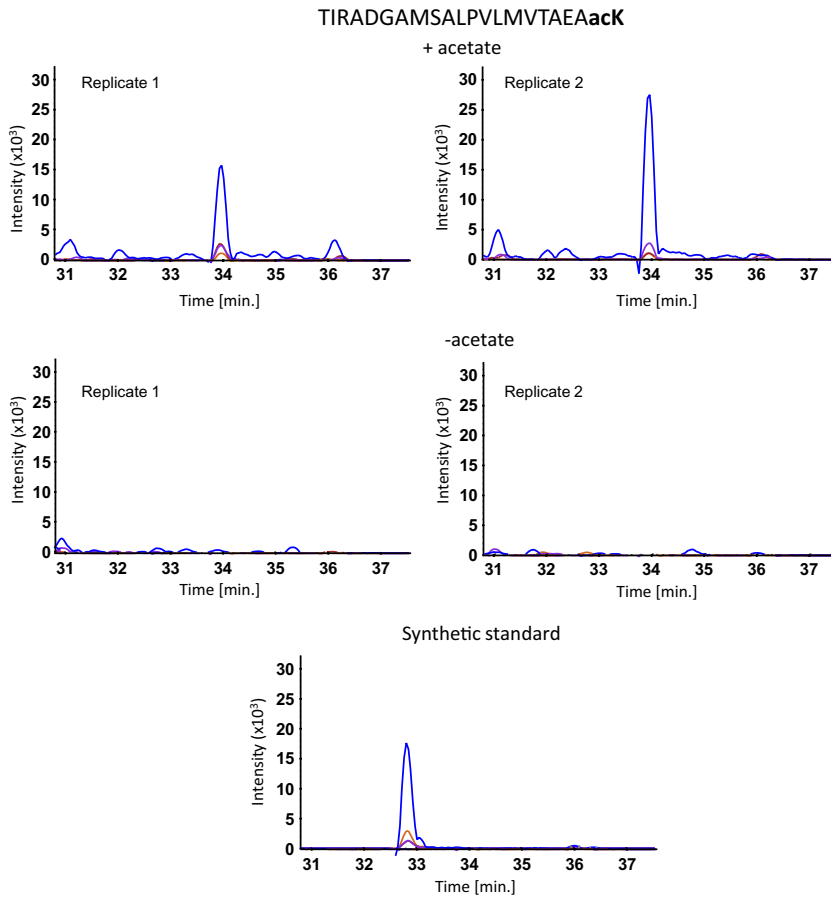


Fig. 1. SRM mass spectrometry analysis of the acetylated peptide TIRADGAMSALPVLMTAEAcK. The plots show overlaid chromatograms of the measured SRM transitions (product ions): b11 (blue), y10 (orange), b14 (purple) and b15 (red). The synthetic standard was external (not spiked directly into the sample), hence the slightly different retention time from the native peptide.

Cells expressing CheY(K91R) and CheY(K109R) were significantly different from cells expressing wild-type CheY or CheY with arginine replacements at other lysine positions. Cells expressing CheY(K91R) spent twice as much time in clockwise rotation as did cells expressing wild-type CheY. Cells expressing CheY(K109R), consistent with earlier observations (Lukat *et al.*, 1991; Bourret *et al.*, 1993), exhibited almost no clockwise rotation

(Fig. 3A). All strains used in this experiment were verified to express CheY to similar levels (Fig. S1). Cells expressing CheY(K91R) and cells expressing CheY(K109R) were also exceptional when flagellar rotation was measured after acetate addition: Cells expressing CheY(K91R) doubled the time spent in clockwise rotation, and cells expressing CheY(K109R) continued rotating counterclockwise almost exclusively (Fig. 3A).

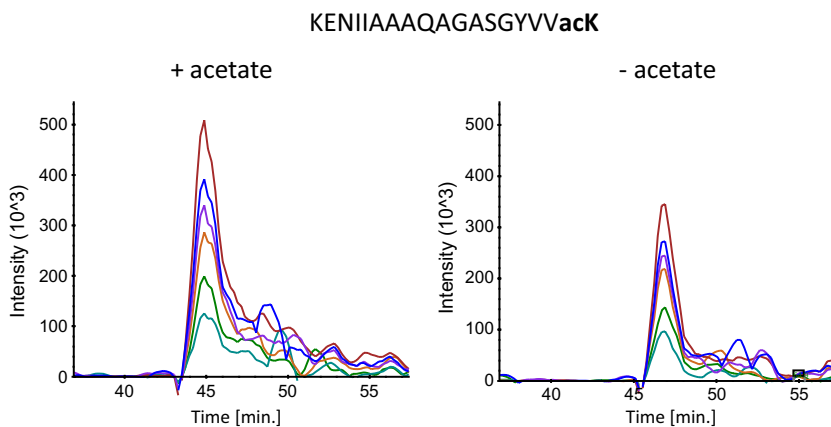


Fig. 2. Targeted parallel reaction monitoring analysis of acetylated peptides using high-resolution mass spectrometry. Presented are overlaid chromatograms of the product ions from peptide KENIIAAAQAGASGYVAcK: b5 (blue), b6 (purple), b7 (red), b9 (orange), b11 (turquoise) and b12 (green). Unlike the SRM experiments, in this analysis, there were no synthetic standards; thus, only relative quantification was performed.

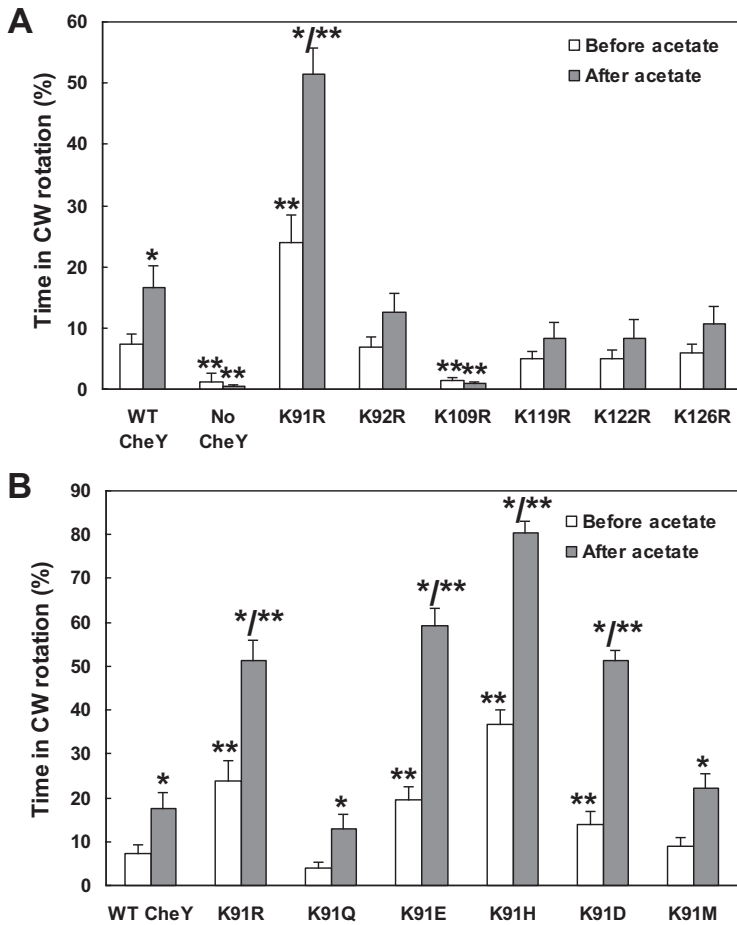


Fig. 3. Acetate-dependent clockwise generation by CheY containing single replacements.

A. KR replacements at the known acetylation sites.

B. Various replacements of K91. All plasmids were expressed (without IPTG) in gutted RBB1097 background to a similar level (Fig. S1C). The direction of flagellar rotation was determined for 1 min prior to, and 10 s subsequent to, addition of acetate (100 mM, pH 7.0). The results are the mean \pm SEM of at least three independent experiments (the number of experiments was determined on the basis of the criterion that additional experiments did not change the mean).

* $P < 0.05$ for the difference between before and after acetate treatment, determined by paired *t*-test. ** $P < 0.05$ for the difference between the mutants and the wild-type control, determined by ANOVA with Dunnett Multiple Comparison Test as post-test.

The other single KR replacements did not significantly affect rotation behavior. These observations, taken together with the mass spectrometry results pointing to K91 and K109 as the major sites that undergo acetylation in response to acetate, suggest that K91 and K109 are the main players in generating clockwise rotation.

K91 likely represses CheY activation

To determine whether the observed clockwise rotation enhancement in cells expressing CheY(K91R) (Fig. 3A) is specific for K replacement by R, we studied additional K replacements at position 91. Clearly, K replacements by H, E and D were at least as effective as R in enhancing clockwise rotation (Fig. 3B). In contrast, K replacements by Q and M were not effective, and the strains behaved like cells expressing wild-type CheY. Notably, the effect of K91R mutation could only be seen in gutted cells expressing CheY, not in wild-type, $\Delta cheY$ cells expressing CheY (Fig. S4). One possible explanation is that the effect of K91R can only be observed when most of CheY is not CheA bound at the receptor complex. [In wild-type cells,

CheY localizes to the cell poles in a CheA-dependent manner (Sourjik and Berg, 2000).]

Two major generalizations can be made from these results. One is that the differences between the K91 replacement mutants are in the basal level of clockwise rotation (i.e., prior to acetate addition). Acetate roughly doubled the clockwise level in all these mutants. The other generalization is that none of the mutations was inhibitory. They either activated CheY to generate more clockwise rotation or had no effect compared with wild-type CheY. This suggests that nonmodified K91 represses to some extent the clockwise-generating activity of the protein, and acetylation of K91 or its replacement by specific amino acids removes this repression, resulting in enhanced clockwise rotation.

To test this conclusion, we constructed a set of multiple mutants in which one of the six acetylation sites was not modified (additional to K109, which we did not modify to enable clockwise generation), while the other four sites were KR replaced. Evidently, only when K91 was not replaced, clockwise rotation was significantly lower than in the wild-type control both before and after acetate addition (Fig. 4A).

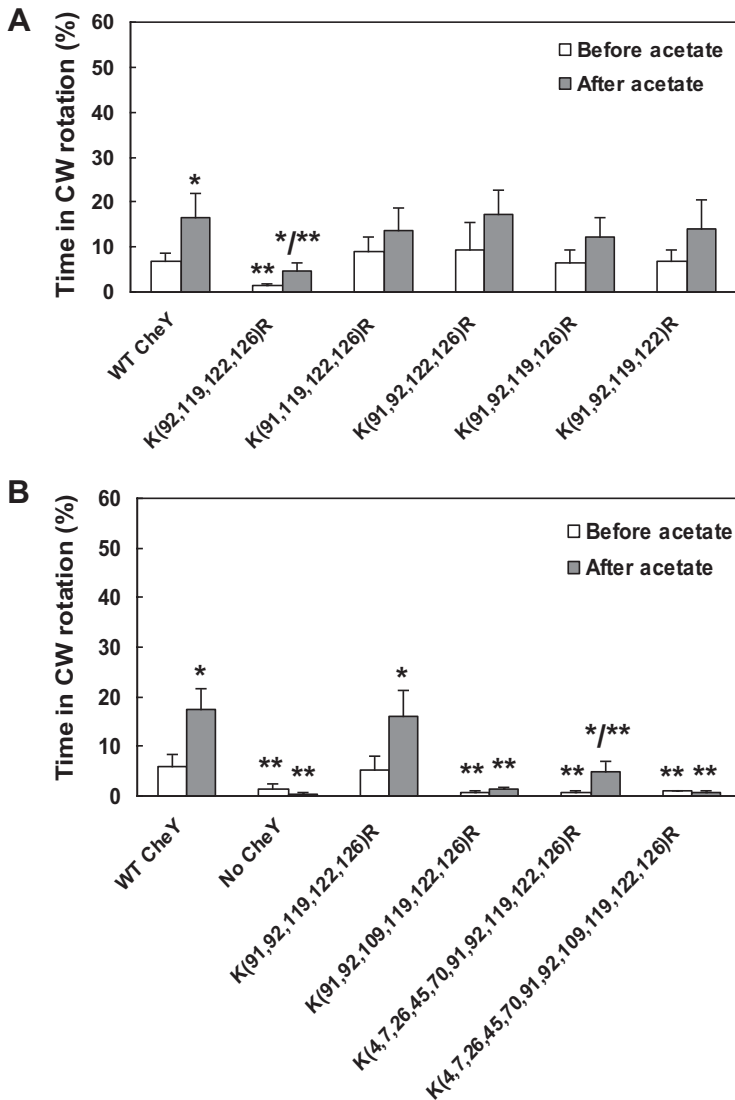


Fig. 4. Acetate-dependent clockwise generation by CheY containing multiple replacements.

A. Mutants expressing CheY protein with four KR replacements each.

B. Multiple KR replacements. All CheY proteins were expressed (without IPTG) in gutted RBB1097 background to a similar level, excluding the proteins with 10 and 11 KR replacements (see text for details). The direction of flagellar rotation was determined before and after (1 min and 10 s respectively) the addition of acetate (100 mM, pH 7.0). The results are the mean \pm SEM of at least three independent experiments (the number of experiments was determined on the basis of the criterion that additional experiments did not change the mean). * $P < 0.05$ for the difference between before and after acetate treatment, determined by paired *t*-test.

** $P < 0.05$ for the difference between the mutants and the wild-type control, determined by ANOVA with Dunnett Multiple Comparison Test as post-test.

By way of elimination: K109 acetylation likely activates CheY

The observations that, in all the cells containing CheY with K91 replacements, addition of acetate roughly doubled the fraction of time spent in clockwise rotation (Fig. 3B) indicate that acetylation of a site other than K91 generates clockwise rotation in these cells. The best candidate for this function is K109. This is for two reasons. First, it is the only site, other than K91, identified to undergo acetate-dependent acetylation *in vivo* (Fig. 2). Second, a mutation in a clockwise-generating site is expected to reduce the clockwise level. From all the single KR replacement mutants, only the one expressing CheY(K109R) exhibited this phenotype (Fig. 3A). To examine the validity of this possibility, we constructed a set of multiple mutants having KR replacements additional to the one in site 91. Because the mass spectrometry results demonstrated

that lysine residues other than those identified earlier can be occasionally acetylated as well (Tables 1 and 2), we also constructed mutants with all 11 lysine residues, or all of them but K109, replaced by arginine (termed hereafter x11KR and x10KR mutants respectively). Clearly, the presence of K109 (i.e., avoiding replacement at this site) enabled the response to acetate, irrespective of which other sites were replaced (Fig. 4B). These observations and the generation of clockwise rotation by acetate even in the x10KR mutant endorse the possibility that acetylation of K109 is the cause of clockwise generation.

A possible role for position 91 in the repression of CheY activation

Generally speaking, because the K91-activating mutations were different from each other in their side chains (includ-

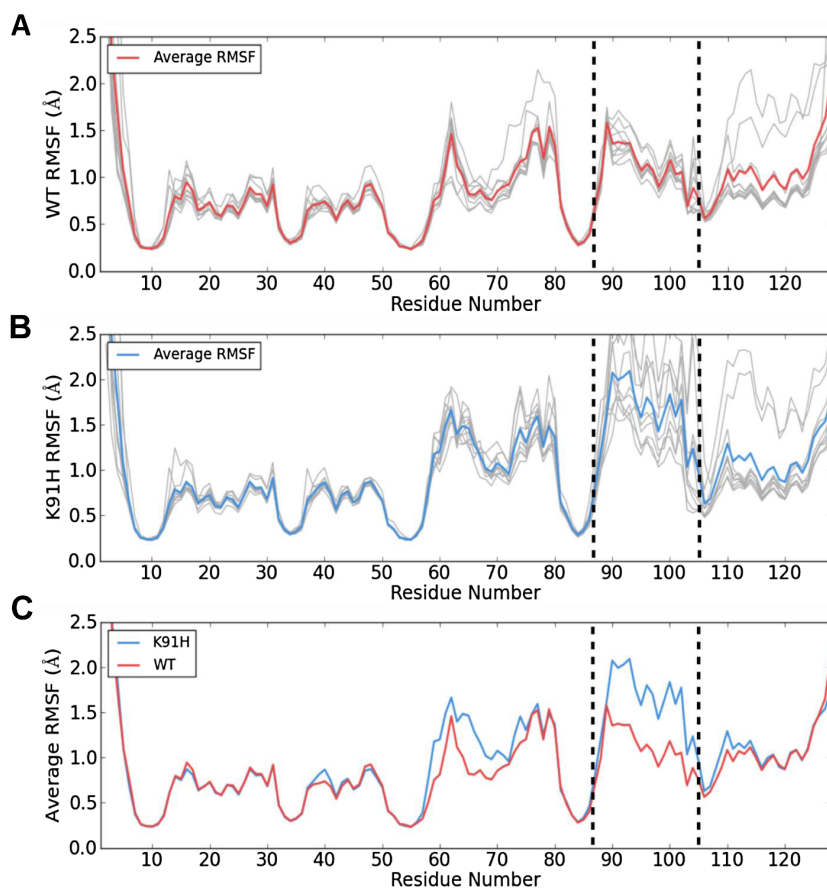


Fig. 5. K91H exhibits high flexibility of $\beta 4\alpha 4$ loop. RMSF versus residue number for wild-type (WT; A) and K91H (B) ensemble simulations. Individual RMSF traces for the ten 250 ns simulations in each ensemble (gray lines) were averaged to produce a mean RMSF value for all 129 CheY residues (colored lines). Overlaying the averaged RMSF traces from the wild-type and K91H ensembles (C) highlights regions of differing stiffness. Vertical dotted lines emphasize the increased flexibility in regions of CheY surrounding the K91 mutation (residues 88–105), including the $\beta 4\alpha 4$ loop (residues 88–91).

ing volume and charge), it is likely that their activating effect is produced by the exclusion of lysine from position 91. To examine how lysine exclusion from position 91 can affect CheY activation at the molecular level, we used all-atom molecular dynamics (MD) simulations for studying the effect of the K91H mutation (shown above to give rise to the most hyperactive phenotype, i.e., the least repressed) on activation and compared it with wild-type CheY. Initial atomic coordinates for both the K91H (with histidine protonated at the δ position) and wild-type CheY models were derived from the crystal structure of *E. coli* CheY (PDB 3CHY) (Volz and Matsumura, 1991). Each system was minimized along with solvent and equilibrated for 250 ns. An ensemble of 10, statistically independent, 250 ns production simulations were subsequently carried out on both the K91H and wild-type systems, resulting in a total of 2.75 μ s of sampling for each model. These simulations revealed a higher level of flexibility in the protein regions surrounding position 91 of the K91H system. In particular, residues 88–102, corresponding to the $\beta 4\alpha 4$ loop and $\alpha 4$ helix, showed, on average, an increase in their root mean squared fluctuations (RMSFs) as compared with the corresponding regions in the ensemble of wild-type simulations (Fig. 5). Based on this result, we hypothesized that

the K91H mutation might give rise to a hyperactive phenotype by altering the conformational dynamics of the $\beta 4\alpha 4$ loop, a region previously shown to correlate with CheY activation (Knaggs *et al.*, 2007; Ma and Cui, 2007; Mottonen *et al.*, 2010).

To characterize the effect of increased flexibility in the protein regions surrounding K91 on the conformational sampling of the $\beta 4\alpha 4$ loop, we used principal components analysis (PCA) (Bishop, 2006) to provide a concise description of the $\beta 4\alpha 4$ loop conformations witnessed by our MD simulations. The utility of the reduced PCA description to capture the salient features of the dynamics of the $\beta 4\alpha 4$ loop was demonstrated by the relatively small number of principal components (PCs) required to describe a significant degree of the conformational variability within the simulation trajectories (Table S3) (Skjaerven *et al.*, 2011). In the present application, the cumulative fractional variance of the top three PCs accounted for over 75% of the total trajectory variance, providing a practical, low-dimensional subspace on to which to project the individual $\beta 4\alpha 4$ loop conformations observed in the K91H and wild-type ensemble simulations. The resulting projections, along with projections of the analogous portions of existing activated CheY structures

(PDBs 1FQW, 1ZDM, 1F4V, 1DJM) and the equilibrated, inactive CheY structure, revealed two well-defined clusters of $\beta 4\alpha 4$ loop conformations (Fig. S5). Notably, $\beta 4\alpha 4$ loop conformations from both the K91H and wild-type simulations inhabited either cluster, while the active and inactive $\beta 4\alpha 4$ loop conformations localized to single clusters opposite to one another (Fig. S5). This suggests that both the K91H and wild-type systems sampled distinct functional states corresponding to the active and inactive $\beta 4\alpha 4$ loop conformations in our MD simulations.

To characterize the organization of projected $\beta 4\alpha 4$ loop conformations in three-dimensional PC space, we used the K-means clustering algorithm (Bishop, 2006) to systematically assign loop conformations to two clusters (Fig. S6). Strikingly, K-means revealed that over 80% of the K91H loop conformations were assigned to the same cluster as the activated loop structures, whereas only <30% of wild-type loop conformations were assigned to this cluster (Table S4). To further survey the distribution of the conformations in 3D PC space, the root mean squared deviation (RMSD) between projections of the activated $\beta 4\alpha 4$ loop conformations and those arising within the K91H mutant and wild-type ensemble simulations was calculated (see *Experimental Procedures*). The resulting cumulative RMSD distributions (Fig. 6) clearly demonstrated an asymmetry in the occupation of the active and inactive $\beta 4\alpha 4$ loop states by the K91H and wild-type CheY systems in agreement with the K-means result. Taken together, the results from our MD simulations and accompanying analysis suggest that the increased flexibility in the $\beta 4\alpha 4$ loop and $\alpha 4$ helix associated with the K91H mutation gives rise to a structural population shift in which the $\beta 4\alpha 4$ loop fluctuates more often near the conformation typical of activated loop structures. It is highly likely that K91 acetylation has an equivalent function in CheY activation. Whether or not this is the case will be the subject of a future study.

Discussion

In this study – the first to identify the acetylation sites on CheY *in vivo* and the first to quantify their acetylation levels – we addressed the question of which of these sites are responsible for acetate-dependent clockwise generation. The main findings made are that K91 and K109 are the predominant sites that undergo acetylation in response to acetate and that these are the sites mainly responsible for the acetate-dependent clockwise generation. The study was carried out with gutted cells in order to avoid perturbations from the phosphorylation system. This means that the results and conclusions are solely relevant to the mechanism of acetylation-dependent clockwise generation.

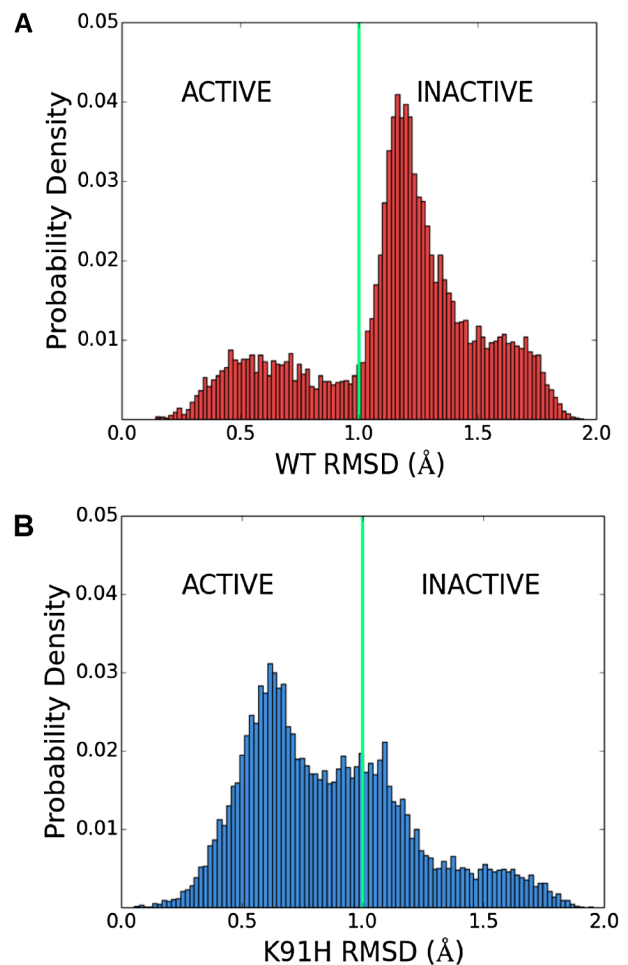


Fig. 6. K91 represses the active state of CheY's $\beta 4\alpha 4$ loop. Distributions of root mean squared deviations (RMSDs) between projections of an activated $\beta 4\alpha 4$ loop structure (PDB 1FQW) and conformations of the $\beta 4\alpha 4$ loop sampled in the wild-type (WT; A) and K91H (B) ensemble simulations. Vertical green lines indicate the rough boundary between clusters in principle component space computed using K-means and highlight the population shift incurred by the K91H mutation. See *Experimental Procedures* for more details.

K91 and K109 are the major sites responsible for acetate-dependent acetylation and clockwise generation

Using SRM mass spectrometry in conjunction with synthetic, acetylated peptide standards, we were able to obtain absolute quantification of the targeted acetylated peptides. One potential drawback of the approach was the fact that peptide concentrations were obtained from in-gel digestion and, therefore, did not reflect the concentration in the sample. Nevertheless, the concentrations still provided an accurate account of the acetylation sites that responded to acetate stimulation. This information combined with high-resolution targeted mass-spectrometry measurements pointed to K91 and K109 as the major sites that

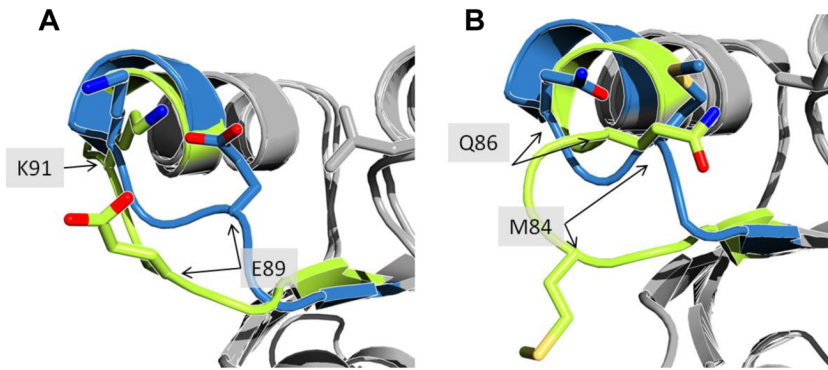


Fig. 7. The equivalent of position 91 plays a role in $\beta 4\alpha 4$ loop repression in CheY from *Thermotoga Maritima*. Aligned structures of active (blue) and inactive (green) conformations of CheY from *E. coli* (A; PDBs 2BJJ and 3CHY) and *Thermotoga Maritima* (B; PDBs 4IGA and 4TMY). The structures were visualized and aligned by PyMOL (The PyMOL Molecular Graphics System, Version 1.5.0.4 Schrödinger, LLC). See text for details.

undergo acetate-stimulated acetylation *in vivo*. These two sites are also the ones found to be autoacetylated *in vitro* (Li *et al.*, 2010). In addition, the responses of tethered cells expressing CheY proteins with a variety of KR replacements (Fig. 3) indicated that K91 and K109 are the sites responsible for acetate-dependent clockwise generation. The rules that emerge from these studies are that K91 must be replaced (by specific amino acids) and K109 must not be replaced for obtaining higher clockwise rotation before or after acetate stimulation (Figs 3A and 4B).

K91 function in acetate-dependent clockwise generation

The observations that clockwise rotation is low whenever K91 is not replaced suggest that K91 represses clockwise rotation. Removal of this repression can apparently be done by two means. One, a physiological mean, is acetylation of K91. The other, an artificial mean, is elimination of K91 by a specific replacement. Obviously, the replacement is more effective than acetylation [see, for example, the much lower clockwise generation by acetate when K91 is not in CheY[K(92,119,122,126)R compared with when K is replaced at position 91 in CheY[K(91,92,119,122,126)R: Fig. 4A and B respectively] because the replacement is on every CheY molecule, whereas acetylation only occurs in a fraction of the CheY molecules (Yan *et al.*, 2008). The effective replacements were K91R, K91H, K91E and K91D. K91Q and K91M replacements were not effective (Fig. 3B).

MD simulations demonstrated that the $\beta 4\alpha 4$ loop of wild-type CheY co-exists in active and inactive states, spending more time in the inactive state (Fig. 6A). The simulations further demonstrated that when K91 is replaced by histidine, the loop spends much more time in the active state (Fig. 6B). Since the K91-activating mutations were different from each other in their side chains and since K91 acetylation is phenotypically similar to K91H replacement, we suggest that the effect of K91 acetylation is mechanistically similar to K91H replacement. This possibility as well as the role of $\beta 4\alpha 4$ loop in the generation of

clockwise rotation and the exact regulatory mechanism of loop flexibility should still be studied.

We further suggest that the mechanism of $\beta 4\alpha 4$ repression has a fundamental role in the regulation of CheY activity. A similar mechanism can apparently be observed in the crystal structures of the active and inactive forms of CheY of *Thermotoga maritima*, in which the $\beta 4\alpha 4$ loop was reported to have a mechanism of activation similar to that of CheY in *E. coli* (Mottonen *et al.*, 2010). The equivalence of *E. coli* K91 (K91^{EC}) in *T. maritima* is Q86 (Q86TM; compare Fig. 7A and B). In the inactive form of the protein, Q86TM blocks the space that, in the active form, is occupied by Y84TM (the equivalent of E89^{EC}) (Fig. 7B). Such an interaction should enhance the stability of the $\beta 4\alpha 4$ loop in its inactive conformation and inhibit the conformational shift to the active form by preventing the burial of Y84TM near the phosphorylation pocket. We interpret the clear interactions of Q86TM in the inactive state *versus* the likely weaker interactions involved in the function of K91^{EC} (Fig. 7A) as an evolutionary temperature adaptation of CheY in *T. maritima*. This adaptation possibly allows the regulation mechanism of CheY activation to be sustained at higher temperatures. In *E. coli* phosphorylation-dependent signaling, a possible role for K91 acetylation may be the prolongation of the lifespan of CheY's active state in a similar manner to the role of E89^{EC} in CheY's autophosphorylation reaction (Thomas *et al.*, 2013).

K109 function in acetate-dependent clockwise generation

Earlier studies, in which any tested replacement of K109 by another amino acid resulted in loss of clockwise rotation (Lukat *et al.*, 1991; Bourret *et al.*, 1993), taken together with our observation that all K109R replacement mutants failed to support clockwise rotation, indicate that K109 is essential for clockwise rotation. Conversely, the observations that the x10KR mutant was capable of exhibiting acetate-dependent clockwise generation (Fig. 4B) and that K109 is one of the two acetylation sites

Table 4. Strains and plasmids used in this study.

	Relevant genotype	Source/reference
Strains		
AG1	<i>recA1 endA1 gyrA96 thi-1 hsdR17(r_Km_K⁺) supE44 relA1</i>	Stratagene
JW1871	AG1+ pCA24N	Kitagawa <i>et al.</i> (2005)
XL-1 Blue	<i>recA1 endA1 gyrA96 thi-1 hsdR17 supE44 relA1 lac</i> [F' <i>proAB lacIqZΔM15 Tn10</i> (Tet ^R)]	Stratagene
UU1631	Δ(<i>cheY</i>) Δ <i>thr</i> (Am)-1 <i>leuB6 his-4 metF</i> (Am)159 <i>eda-50 rpsL136 Strep^R</i> [thi-1 <i>ara-14 lacY1 mtl-1 xyl-5 tonA31 tsx-78</i>]	VS100 in Sourjik and Berg (2000)
RBB1097	CP875 Δ(<i>cheA</i> – <i>cheZ</i>)::Zeocin ^R , Δ(<i>ackA pta hisJ hisP dhu</i>) <i>zej-223::Tn10</i>	Barak <i>et al.</i> (1998)
EW289	UU1631 + pCA24N (<i>cheY</i>)	This study
EW330	RBB1097 + pCA24N (<i>cheY</i>)	This study
EW333	RBB1097 + pCA24N [<i>cheY</i> (K92,119,122,126R)]	This study
EW334	RBB1097 + pCA24N [<i>cheY</i> (K91,92,119,122,126R)]	This study
EW335	RBB1097 + pCA24N [<i>cheY</i> (K91R)]	This study
EW336	RBB1097 + pCA24N [<i>cheY</i> (K92R)]	This study
EW337	RBB1097 + pCA24N [<i>cheY</i> (K109R)]	This study
EW338	RBB1097 + pCA24N [<i>cheY</i> (K119R)]	This study
EW339	RBB1097 + pCA24N [<i>cheY</i> (K122R)]	This study
EW340	RBB1097 + pCA24N [<i>cheY</i> (K126R)]	This study
EW411	RBB1097 + pCA24N [<i>cheY</i> (K4,7,26,45,70,91,92,119,122,126R)]	This study
EW415	RBB1097 + pCA24N [<i>cheY</i> (K4,7,26,45,70,91,92,109,119,122,126R)]	This study
EW418	RBB1097 + pCA24N [<i>cheY</i> (K91,92,109,119,122,126R)]	This study
EW451	RBB1097 + pCA24N [<i>cheY</i> (K91,92,122,126R)]	This study
EW455	RBB1097 + pCA24N [<i>cheY</i> (K91,92,119,122R)]	This study
EW465	RBB1097 + pCA24N [<i>cheY</i> (K91,119,122,126R)]	This study
EW466	RBB1097 + pCA24N [<i>cheY</i> (K91,92,119,126R)]	This study
EW547	RBB1097 + pCA24N [<i>cheY</i> (K91Q)]	This study
EW588	RBB1097 + pCA24N [<i>cheY</i> (K91E)]	This study
EW590	RBB1097 + pCA24N [<i>cheY</i> (K91H)]	This study
EW595	RBB1097 + pCA24N [<i>cheY</i> (K91M)]	This study
EW596	RBB1097 + pCA24N [<i>cheY</i> (K91D)]	This study
Plasmid		
pCA24N	CheY-His ₆ overexpression, chloramphenicol resistance	Kitagawa <i>et al.</i> (2005)

that undergo acetate-stimulated enhancement of the acetylation level *in vivo* (Fig. 2) suggest that acetylation of K109 generates CW rotation. As just discussed, this clockwise generation can mainly be observed when K91 is replaced or acetylated.

Yet the gutted strain expressing CheY x10KR mutant protein spent less time in clockwise rotation than that expressing wild-type CheY (Fig. 4B). The reason for this is, at least in part, the much-reduced expression levels of the x10KR and x11KR CheY mutant proteins relative to all other strains (right panel in Fig. S1C). This reduced expression was probably due to the lower solubility of the x10KR and x11KR proteins, evident from the formation of inclusion bodies when they are produced. Consistent with this explanation, the mutant CheY[K(91,92,119,122,126)R], which lacks all the acetylation sites except for K109, had wild-type-like rotation.

Earlier studies that observed the inability of cells expressing CheY(K109R) to generate clockwise rotation attributed this flaw to breaking presumably important intramolecular interactions of K109 (Bourret *et al.*, 1993). Thus, it was suggested that K109 may form a salt bridge with Asp-57 of nonphosphorylated CheY (Silverman and Simon, 1974; Volz and Matsumura, 1991) and that it may

be involved in coordinating one of the oxygen atoms of the phosphoryl group on CheY (Robinson *et al.*, 2000). Yet the observations that CheY(K109R) is hyperphosphorylated (Lukat *et al.*, 1991) and that K109 is apparently uninvolved in phosphotransfer catalysis (Silversmith *et al.*, 1997), taken together with the fact that all our results were obtained in gutted cells lacking the phosphorylation system and the enzymes that convert acetate to acetyl phosphate, strongly argue that the ability of K109 acetylation to generate clockwise rotation is phosphorylation independent. The mechanism by which K109 activates CheY is still largely unknown. Once the function of K109 in activating CheY is fully understood, the mechanism by which K109 acetylation activates the protein can be resolved.

Experimental procedures

Bacterial strains and plasmids

The *E. coli* strains, plasmids and primers used in this study are listed in Table 4 and Table S5. All mutants were generated by site-directed mutagenesis derived from a polymerase chain reaction, using an appropriate set of primers and, as a template, a pCA24N vector carrying wild-type *cheY* with

N-terminal His-tag from the ASKA library (Kitagawa *et al.*, 2005). The resulting recombinant plasmids were introduced into *E. coli* XL-1 Blue cells and then isolated using a plasmid purification kit (QIAGEN) and sequenced. All DNA manipulations and standard molecular biology protocols were performed as described (Sambrook and Russell, 2001).

Quantitative LCMS analyses

Gutted *E. coli* cells of strain UU1631 expressing 6xHis-CheY from a plasmid were grown at 37°C on tryptone broth supplemented with chloramphenicol (Sigma, Israel; 34 µg ml⁻¹) to O.D.₅₉₀ = 0.9 with or without induction of IPTG (1 mM). One hour before harvesting, the culture was divided into two equal portions, one incubated with sodium acetate (100 mM; pH 7.0; Merck) and the other without acetate. The harvested cells were washed twice with motility buffer [10 mM potassium phosphate buffer (pH 7.0), 0.1 mM EDTA and 0.1 mM L-methionine (Adler, 1973)], lysed by BugBuster (Novagen) and subjected to SDS-PAGE 12%. The CheY bands were cut from the gel and destained. Proteins were then reduced by incubation with dithiothreitol (5 mM; Sigma) for 30 min at 60°C and alkylated with 10 mM iodoacetamide (Sigma) in the dark for 30 min at 21°C. Proteins were then subjected to digestion with trypsin (Promega, Madison, WI, USA) or to digestion with chymotrypsin (Sigma Aldrich, St. Louis, MO, USA) for 6 h followed by trypsin for 16 h at 37°C. The digestions were stopped by trifluoroacetic acid (1%). The samples were stored in -80°C.

Liquid chromatography

ULC/MS-grade solvents were used for all chromatographic steps. Each sample was loaded using splitless nano-Ultra Performance Liquid Chromatography (10 kpsi nanoAcquity; Waters, Milford, MA, USA). The mobile phase was (i) H₂O + 0.1% formic acid and (ii) acetonitrile + 0.1% formic acid. Desalting of the samples was performed online using a reversed-phase C18 trapping column (180 µm internal diameter, 20 mm length, 5 µm particle size; Waters). The peptides in the samples were separated using a C18 T3 HSS nano-column (75 µm internal diameter, 150 mm length, 1.8 µm particle size; Waters) at 0.4 µl min⁻¹. Peptides were eluted from the column into the mass spectrometer using the following gradient: 3–30%ii in 30 min, 30–95%ii in 5 min, maintained at 95% for 7 min and then back to initial conditions.

Low-resolution mass spectrometry

The nanoLC was coupled online through a nanoESI emitter (7 cm length, 10 mm tip; New Objective; Woburn, MA, USA) to a tandem quadrupole mass spectrometer (Xevo TQ-S, Waters Corp.). Data were acquired in SRM using MASSLYNX 4.1 (Waters, Milford, MA, USA). In the high-resolution-targeted analysis, the nanoLC was coupled to a quadrupole Orbitrap mass spectrometer (Thermo Scientific) and operated in 'targeted MS2' mode.

High-resolution mass spectrometry

The nanoLC was coupled online through a Flexlon nanospray using a nanoESI emitter (7 cm length, 10 mm tip; New Objec-

tive) to a quadrupole orbitrap mass spectrometer (Q Exactive, Thermo Scientific). The mass spectrometer was operated in Parallel Reaction Monitoring mode (Peterson *et al.*, 2012). Orbitrap resolution was set to 35,000; automatic gain control target was set to 2e5 and injection time to 250 ms.

Data analysis

Raw data were then imported into SKYLINE software (MacLean *et al.*, 2010) for final processing and evaluation. Quantification was based on the area under the curve of extracted ion chromatogram from the most intense transition per peptide. At least three overlapping SRM transitions were acquired per peptide. Acetylated peptides were synthesized (JPT, Germany) and ran prior to the samples for use as external standards (Table S1). The signal from the native peptides was referenced to the standards to obtain absolute concentrations.

Acetate-dependent clockwise generation

For studying acetate-dependent clockwise generation, plasmids expressing wild-type or mutant CheY proteins (listed in Table 4) were introduced into the gutted strain RBB1097 lacking all the genes from *cheA* to *cheZ* and also deleted for *ack* and *pta* (Table 4). These strains, lacking all the chemotaxis proteins, some of the chemotaxis receptors, and the enzymes that convert acetate to AcCoA via acetyl phosphate and *vice versa*, were grown at 37°C on tryptone broth supplemented with chloramphenicol (34 µg ml⁻¹) to O.D.₅₉₀ = 0.7. These cells expressed the plasmids listed in Table 4 even though they were grown without IPTG induction due to leakiness of the plasmids. To determine the direction of flagellar rotation and the response to acetate, we used the tethering assay (Silverman and Simon, 1974). Cells were washed twice and resuspended in a motility buffer containing 10 mM potassium phosphate (pH 7.0), 0.1 mM EDTA and 0.1 mM L-methionine (Adler, 1973). The cells were tethered through their flagella to glass slides in a flow chamber (Berg and Block, 1984) as described earlier (Ravid and Eisenbach, 1983), and the rotation of the tethered cells (at room temperature, 23–25°C) was recorded and analyzed using home-made computer software. When needed, acetate (100 mM; pH 7.0) was added in the motility buffer to the flow chamber.

Estimation of CheY expression levels in ΔcheY strains

Cells of each strain were grown to midexponential phase (OD₅₉₀ = 0.6) and divided into two portions. IPTG (1 mM) was added to one of the portions, and both portions were further incubated at 37°C for 3 h. Cell-free extracts were prepared by BugBuster according to manufacturer instructions and subjected to SDS-PAGE (12% polyacrylamide) followed by Western blots with an anti-6xHis antibody.

Statistical analysis

All statistical analyses were carried out using INSTAT 3 software package (Graph Pad Software, USA).

MD simulations

System setup. Atomic coordinates for the initial wild-type and K91H CheY protein models were taken from the crystallographically derived PDB 3CHY (Volz and Matsumura, 1991). For residues in the PDB in which multiple orientations of the side chains were present, the conformation with the highest reported occupancy was taken. Water molecules present in the PDB were also retained. In the case of the K91H CheY model, lysine 91 was replaced with a histidine protonated at the δ position using the psfgen module in VMD (Humphrey *et al.*, 1996). Models were then hydrated with TIP3P water molecules using VMD's solvate plugin, resulting in a simulation box of size 64 by 59 by 60 Å. Using VMD's autoionize plugin, the wild-type and K91H systems were then neutralized by adding four and five sodium ions, respectively, and subsequently ionized with sodium and chloride ions to the physiological concentration of 150 mM. The resulting wild-type and K91H systems contained 21,191 and 21,193 atoms, respectively, including protein, water and ions.

Simulation protocol. All MD simulations were performed using the parallel MD code, NAMD 2.9 (Phillips *et al.*, 2005; Mei *et al.*, 2011), and CHARMM22 force field (MacKerell *et al.*, 1998). Simulations were conducted in the NPT ensemble with isobaric and isothermal conditions maintained at 1 atm and 310°K using the Nosé-Hoover Langevin piston with period 200 fs and decay 50 fs and the Langevin thermostat with a temperature coupling of 5 ps⁻¹. The r-RESPA integrator scheme (Phillips *et al.*, 2005) with an integration time step of 2 fs was used in all simulations. SHAKE constraints were applied to all hydrogen atoms (Ryckaert *et al.*, 1977). Short-range, nonbonded interactions, calculated every 2 fs with a cutoff of 12 Å and long-range electrostatics, were evaluated every 6 fs using the particle mesh Ewald method (Darden *et al.*, 1993) with a grid size of 1 Å. Periodic boundary conditions were used in all simulations. Both wild-type and K91H models were subjected to a series of conjugant gradient energy minimizations: 100,000 steps with all protein atoms excluding hydrogen restrained, 100,000 steps with backbone atoms restrained and 100,000 steps with all atoms unrestrained. Before proceeding with unrestrained equilibration simulations, each model underwent a 2 ns NPT simulation in which backbone atoms were harmonically restrained with spring constant = 0.5 kcal mol⁻¹ × nm².

Simulation analysis. Visualization and extraction of raw trajectory data for analysis were performed using VMD (Humphrey *et al.*, 1996). RMSF calculations were performed using the *measure* function in VMD (Humphrey *et al.*, 1996). Clustering analysis was performed using the implementation of the K-means algorithm from the python scientific computing library, Scipy (Jones *et al.*, 2001). PCA was performed using the protein dynamics analysis package, ProDy (Bakan *et al.*, 2011). Before conducting PCA, the backbone atomic coordinates of the $\beta 4\alpha 4$ loop (residues 88–91) were extracted from the concatenated K91H and wild-type ensemble simulations and aligned using root mean square deviation fitting in VMD. A total of 25,000 conformations (12,500 per model), sampled over 5 μ s of simulation, were analyzed. The top three resulting PCs were used as a basis on which the

backbone structures of the $\beta 4\alpha 4$ loop were projected for further analysis. The RMSD values depicted in Fig. 6 were calculated in the three-dimensional PC space described above and are equivalent to the Euclidean distances between projections of a representative activated loop conformation (PDB 1FQW) and those arising in the K91H and wild-type ensemble simulation trajectories. Illustrations of K-means and PCA results were produced using the python plotting library, Matplotlib (Hunter, 2007).

Acknowledgements

We thank the Smoler Proteomics Research Center of the Technion, Haifa, Israel, for carrying out tandem mass spectrometry for the identification of CheY acetylation sites *in vivo*. We also thank Yulian Gavrilov and Dr. Yaakov Levy (Weizmann Institute of Science) for their help with the production and analysis of the MD simulations at the preliminary stage, Olga Khersonsky (Weizmann Institute) for her advice in site-directed mutagenesis, Dr. Leah Armon (Weizmann Institute) for statistical advice, and Dr. Juan R. Perilla and Dr. Wei Han (University of Illinois at Urbana-Champaign) for insightful discussions and advice regarding the computational aspects of this manuscript. M.E. is an incumbent of the Jack and Simon Djanogly Professorial Chair in Biochemistry. This study was supported by grant no. 534/10 from the Israel Science Foundation and by the Minerva Foundation with funding from the Federal German Ministry for Education and Research. Funding was also provided by National Institutes of Health grant No. 9P41GM104601 and National Science Foundation grant No. PHY-1430124. MD simulations were performed on the Blue Waters supercomputer as part of the Petascale Computational Resource (PRAC) grant 'The Computational Microscope', which is supported by the National Science Foundation (award number ACI-1440026).

References

- Addona, T.A., Abbatiello, S.E., Schilling, B., Skates, S.J., Mani, D.R., Bunk, D.M., *et al.* (2009) Multi-site assessment of the precision and reproducibility of multiple reaction monitoring-based measurements of proteins in plasma. *Nat Biotechnol* **27**: 633–641.
- Adler, J. (1966) Chemotaxis in bacteria. *Science* **153**: 708–716.
- Adler, J. (1973) A method for measuring chemotaxis and use of the method to determine optimum conditions for chemotaxis by *Escherichia coli*. *J Gen Microbiol* **74**: 77–91.
- Bakan, A., Meireles, L.M., and Bahar, I. (2011) ProDy: protein dynamics inferred from theory and experiments. *Bioinformatics* **27**: 1575–1577.
- Barak, R., Welch, M., Yanovsky, A., Oosawa, K., and Eisenbach, M. (1992) Acetyladenylate or its derivative acetylates the chemotaxis protein CheY *in vitro* and increases its activity at the flagellar switch. *Biochemistry (USA)* **31**: 10099–10107.
- Barak, R., Abouhamad, W.N., and Eisenbach, M. (1998) Both acetate kinase and acetyl Coenzyme A synthetase are involved in acetate-stimulated change in the direction of flagellar rotation in *Escherichia coli*. *J Bacteriol* **180**: 985–988.

- Barak, R., Prasad, K., Shainskaya, A., Wolfe, A.J., and Eisenbach, M. (2004) Acetylation of the chemotaxis response regulator CheY by acetyl-CoA synthetase from *Escherichia coli*. *J Mol Biol* **342**: 383–401.
- Barak, R., Yan, J., Shainskaya, A., and Eisenbach, M. (2006) The chemotaxis response regulator CheY can catalyze its own acetylation. *J Mol Biol* **359**: 251–265.
- Berg, H.C., and Block, S.M. (1984) A miniature flow cell designed for rapid exchange of media under high-power microscope objectives. *J Gen Microbiol* **130**: 2915–2920.
- Bishop, C.M. (2006) *Pattern Recognition and Machine Learning*. Singapore: Springer Verlag.
- Bourret, R.B., Drake, S.K., Chervitz, S.A., Simon, M.I., and Falke, J.J. (1993) Activation of the phosphosignaling protein CheY. II. Analysis of activated mutants by ¹⁹F NMR and protein engineering. *J Biol Chem* **268**: 13089–13096.
- Darden, T., York, D., and Pedersen, L. (1993) Particle mesh Ewald: an N log (N) method for Ewald sums in large systems. *J Chem Phys* **98**: 10089–10092.
- Eng, J.K., McCormack, A.L., and Yates, J.R. (1994) An approach to correlate tandem mass spectral data of peptides with amino acid sequences in a protein database. *J Am Soc Mass Spectrom* **5**: 976–989.
- Humphrey, W., Dalke, A., and Schulten, K. (1996) VMD: visual molecular dynamics. *J Mol Graph* **14**: 33–38.
- Hunter, J.D. (2007) Matplotlib: a 2D graphics environment. *Comput Sci Eng* **9**: 90–95.
- Jones, E., Oliphant, T., and Peterson, P. (2001) SciPy: open source scientific tools for Python. [WWW document]. URL <http://www.scipy.org/>
- Jones, J.D., and O'Connor, C.D. (2011) Protein acetylation in prokaryotes. *Proteomics* **11**: 3012–3022.
- Kim, G.W., and Yang, X.J. (2011) Comprehensive lysine acetylomes emerging from bacteria to humans. *Trends Biochem Sci* **36**: 211–220.
- Kitagawa, M., Ara, T., Arifuzzaman, M., Ioka-Nakamichi, T., Inamoto, E., Toyonaga, H., and Mori, H. (2005) Complete set of ORF clones of *Escherichia coli* ASKA library (a complete set of *E. coli* K-12 ORF archive): unique resources for biological research. *DNA Res* **12**: 291–299.
- Knaggs, M.H., Salsbury, F.R.J., Edgell, M.H., and Fetrow, J.S. (2007) Insights into correlated motions and long-range interactions in CheY derived from molecular dynamics simulations. *Biophys J* **92**: 2062–2079.
- Li, M., Luo, J., Brooks, C.L., and Gu, W. (2002) Acetylation of p53 inhibits its ubiquitination by Mdm2. *J Biol Chem* **277**: 50607–50611.
- Li, R., Gu, J., Chen, Y.Y., Xiao, C.L., Wang, L.W., Zhang, Z.P., et al. (2010) CobB regulates *Escherichia coli* chemotaxis by deacetylating the response regulator CheY. *Mol Microbiol* **76**: 1162–1174.
- Lukat, G.S., Lee, B.H., Mottonen, J.M., Stock, A., and Stock, J.B. (1991) Roles of the highly conserved aspartate and lysine residues in the response regulator of bacterial chemotaxis. *J Biol Chem* **266**: 8348–8354.
- Ma, L., and Cui, Q. (2007) Activation mechanism of a signaling protein at atomic resolution from advanced computations. *J Am Chem Soc* **129**: 10261–10268.
- MacKerell, A.D., Bashford, D., Bellott, M., Dunbrack, R.L., Evanseck, J.D., Field, M.J., et al. (1998) All-atom empirical potential for molecular modeling and dynamics studies of proteins. *J Phys Chem B* **102**: 3586–3616.
- MacLean, B., Tomazela, D.M., Shulman, N., Chambers, M., Finney, G.L., Frewen, B., et al. (2010) Skyline: an open source document editor for creating and analyzing targeted proteomics experiments. *Bioinformatics* **26**: 966–968.
- Mei, C., Sun, Y., Zheng, G., Bohm, E.J., Kale, L.V., Phillips, C.J., and Harrison, C. (2011) Enabling and scaling biomolecular simulations of 100 million atoms on petascale machines with a multicore-optimized message-driven runtime. 2011 International conference for High performance computing, networking, storage and analysis (SC), pp. 1–11.
- Mottonen, J.M., Jacobs, D.J., and Livesay, D.R. (2010) Allosteric response is both conserved and variable across three CheY orthologs. *Biophys J* **99**: 2245–2254.
- Peterson, A.C., Russell, J.D., Bailey, D.J., Westphall, M.S., and Coon, J.J. (2012) Parallel reaction monitoring for high resolution and high mass accuracy quantitative, targeted proteomics. *Mol Cell Proteomics* **11**: 1475–1488.
- Phillips, J.C., Braun, R., Wang, W., Gumbart, J., Tajkhorshid, E., Villa, E., et al. (2005) Scalable molecular dynamics with NAMD. *J Comput Chem* **26**: 1781–1802.
- Ramakrishnan, R., Schuster, M., and Bourret, R.B. (1998) Acetylation at Lys-92 enhances signaling by the chemotaxis response regulator protein CheY. *Proc Natl Acad Sci U S A* **95**: 4918–4923.
- Ravid, S., and Eisenbach, M. (1983) Correlation between bacteriophage *chi* adsorption and mode of flagellar rotation of *Escherichia coli* chemotaxis mutants. *J Bacteriol* **154**: 604–611.
- Robinson, V.L., Buckler, D.R., and Stock, A.M. (2000) A tale of two components: a novel kinase and a regulatory switch. *Nat Struct Biol* **7**: 626–633.
- Ryckaert, J.-P., Ciccotti, G., and Berendsen, H.J.C. (1977) Numerical integration of the Cartesian equations of motion of a system with constraints: molecular dynamics of n-alkanes. *J Comput Phys* **23**: 327–341.
- Sambrook, J., and Russell, D. (2001) *Molecular Cloning: A Laboratory Manual*, 3rd edn. Cold Spring Harbor, NY: Cold Spring Harbor Laboratory Press.
- Silverman, M., and Simon, M. (1974) Flagellar rotation and the mechanism of bacterial motility. *Nature* **249**: 73–74.
- Silversmith, R.E., Appleby, J.L., and Bourret, R.B. (1997) Catalytic mechanism of phosphorylation and dephosphorylation of CheY: kinetic characterization of imidazole phosphates as phosphodonors and the role of acid catalysis. *Biochemistry (USA)* **36**: 14965–14974.
- Skjaerven, L., Martinez, A., and Reuter, N. (2011) Principal component and normal mode analysis of proteins; a quantitative comparison using the GroEL subunit. *Proteins* **79**: 232–243.
- Sourjik, V., and Berg, H.C. (2000) Localization of components of the chemotaxis machinery of *Escherichia coli* using fluorescent protein fusions. *Mol Microbiol* **37**: 740–751.
- Thao, S., and Escalante-Semerena, J.C. (2011) Control of protein function by reversible N ϵ -lysine acetylation in bacteria. *Curr Opin Microbiol* **14**: 200–204.
- Thomas, S.A., Immormino, R.M., Bourret, R.B., and

- Silversmith, R.E. (2013) Nonconserved active site residues modulate CheY autophosphorylation kinetics and phospho-donor preference. *Biochemistry (USA)* **52**: 2262–2273.
- Volz, K., and Matsumura, P. (1991) Crystal structure of *Escherichia coli* CheY refined at 1.7-Å resolution. *J Biol Chem* **266**: 15511–15519.
- Wolfe, A.J., Conley, M.P., and Berg, H.C. (1988) Acetylade-nylate plays a role in controlling the direction of flagellar rotation. *Proc Natl Acad Sci U S A* **85**: 6711–6715.
- Yan, J., Barak, R., Liarzi, O., Shainskaya, A., and Eisenbach, M. (2008) *In vivo* acetylation of CheY, a response regulator in chemotaxis of *Escherichia coli*. *J Mol Biol* **376**: 1260–1271.

Supporting information

Additional supporting information may be found in the online version of this article at the publisher's web-site.